

5-2007

Velocity half-sphere model for multiple scattering in a semi-infinite medium

S Menon

Illinois State University

Q Su

Illinois State University

Rainer Grobe

Illinois State University

Follow this and additional works at: <https://ir.library.illinoisstate.edu/fpphys>

 Part of the [Atomic, Molecular and Optical Physics Commons](#)

Recommended Citation

Menon, S; Su, Q; and Grobe, Rainer, "Velocity half-sphere model for multiple scattering in a semi-infinite medium" (2007). *Faculty publications – Physics*. 34.

<https://ir.library.illinoisstate.edu/fpphys/34>

This Article is brought to you for free and open access by the Physics at ISU ReD: Research and eData. It has been accepted for inclusion in Faculty publications – Physics by an authorized administrator of ISU ReD: Research and eData. For more information, please contact ISURed@ilstu.edu.

Velocity half-sphere model for multiple scattering in a semi-infinite medium

S. Menon, Q. Su, and R. Grobe

Intense Laser Physics Theory Unit and Department of Physics, Illinois State University, Normal, Illinois 61790-4560, USA

(Received 6 November 2006; published 18 May 2007)

We show how the velocity half-sphere model [S. Menon, Q. Su, and R. Grobe, *Phys. Rev. E* **72**, 041910 (2005)] recently introduced to predict the propagation of light for an infinite turbid medium can be extended to account for the emission of multiply scattered light for a geometry with a planar boundary. A comparison with exact solutions obtained from Monte Carlo simulations suggests that this approach can improve the predictions of the usual diffusion theory for both isotropic and highly forward scattering media with reflecting interfaces.

DOI: [10.1103/PhysRevA.75.053817](https://doi.org/10.1103/PhysRevA.75.053817)

PACS number(s): 42.25.Fx, 87.90.+y, 05.60.-k, 42.62.Be

I. INTRODUCTION

The diffusion theory has become a powerful tool in predicting many phenomena in various branches of science. In astrophysics it describes electromagnetic radiation patterns from stars and galaxies, in nuclear physics it models the emission of neutrons from radioactive materials [1,2], and in statistical mechanics it models Brownian motion. The formalism can be obtained as an approximation to the radiative transfer equation by assuming that the photons (or particles) evolve nearly isotropically throughout the medium [3]. The diffusion model is also widely used to model the scattering of light in biological materials, which is important for recent medical imaging applications [4–6]. This particular interest was fueled by the observation that light in the 600–900 nm wavelength range can propagate up to 10 cm [7–9] without significant attenuation in soft tissues.

Unfortunately, to describe the scattering accurately near the source [10–12] in highly forward scattering media such as biological materials, a direct application of the traditional diffusion theory is problematic as the required isotropy cannot be satisfied. It is especially unreliable close to a physical boundary [13,14], such as an interface between two media with different optical characteristics. As a consequence, several imaging schemes based on this theory become unreliable, as the inverse problem required for imaging is highly nonlinear and any error in the description of light near a boundary can affect the final outcome significantly. One possible solution would be to obtain full solutions to the radiative transfer equation. Unfortunately, there are only few situations for which this equation can be solved exactly [1] and in most cases one has to rely on computational approaches such as CPU time consuming Monte Carlo techniques [15].

The diffusion model has several specific problems associated with physical boundaries. First, as the diffusion theory requires a spherical harmonics expansion of the irradiance with a finite number of terms, the exact boundary condition cannot be imposed and one has to rely on an approximate set of conditions [14,16–21]. Three different types are often used including the zero boundary condition, the partial current condition, and the extrapolated boundary condition [16,17]. Second, the extrapolated boundary condition solution, which is the only real improvement to the diffusion solution, is based on an exact solution to the Milne problem [22] for an isotropically scattering semi-infinite medium with

infinite extension along the transverse direction. This correction has limited usage in bio-optical imaging because of the highly forward scattering nature of tissuelike media and the presence of transverse effects often unavoidable in realistic laboratory setups. Also, as we will show below, this ad hoc empirical correction violates even the norm conservation condition for sources with finite strength. Third, in cases where the interface is index mismatched, the resulting boundary conditions due to reflection cannot be taken adequately into account by the usual diffusion model.

Thus it is desirable to improve the diffusion model for imaging based on surface measurements [13,14]. In a recent work [23], we have extended the traditional diffusion theory by distinguishing between the irradiance in the forward and backward directions at each point in space. This so called velocity half-sphere (VHS) model led to a new effective source for the diffusion equation that can better represent an anisotropic light source. Its predictions differ significantly from the traditional diffusion theory for short source-detector spacings. For an infinite medium without any boundaries, we derived an analytical solution for the two lowest-order velocity moments of the irradiance and referred to an investigation of the boundary effects in a follow-up paper.

In this work, we will show how the VHS model can provide new solutions to the radiative transfer equation to describe the emission from reflecting and nonreflecting boundaries. We will show how the problems listed above can be corrected with this approach. Though, in principle, this approach can be applied to other geometries, we will focus in this work on a semi-infinite turbid medium with a planar boundary.

The paper is organized as follows. In Sec. II we discuss the general problem of imposing exact boundary conditions on a system in which the irradiance is approximated by an expansion in the velocity moments of only finite order. In Sec. III we briefly review the various choices with regard to the boundary conditions for the standard diffusion model. In Sec. IV we outline how these conditions can be improved for the velocity-half sphere model leading to more accurate analytical solutions. In Sec. V we compare the analytical solutions from Secs. III and IV with Monte Carlo solutions obtained for the radiative transfer equation. In Sec. VI we conclude with a brief discussion.

II. THE MODEL SYSTEM

The interaction of light with a highly scattering medium can be modeled macroscopically by the radiative transfer (Boltzmann) equation. In the steady state the phase-space irradiance function $I(\mathbf{r}, \Omega)$ satisfies

$$\begin{aligned} (\Omega \cdot \nabla + \mu_T)I(\mathbf{r}, \Omega) &= \mu_s \int d\Omega' p(\Omega \cdot \Omega') I(\mathbf{r}, \Omega') \\ &+ [q_+ \Theta(\cos \theta) \\ &+ q_- \Theta(-\cos \theta)] \delta(x) \delta(y) \delta(z - z_s) / 2\pi, \end{aligned} \quad (2.1)$$

where $\Omega \equiv (\sin \theta \cos \phi, \sin \theta \sin \phi, \cos \theta)$ is a normalized velocity vector for photons with polar angles (θ, ϕ) , μ_s (μ_a) is the scattering (absorption) coefficient and $\mu_T \equiv \mu_s + \mu_a$. The scattering phase function $p(\Omega \cdot \Omega')$ determines the scattering properties of the medium extending into the half-space $z > 0$. We assume that a point source is located at $z = z_s$ inside the medium and q_+ and q_- are parameters that can take the values between 0 and 1 to model isotropically or anisotropically emitted light. Note that we have separated the source into positive ($q_+ = 1, q_- = 0$) and negative ($q_+ = 0, q_- = 1$) velocity hemispheres with respect to the z axis using the Heaviside unit step function $\Theta(x)$ defined as $\Theta(x) \equiv (1 + |x|/x)/2$. For example, a perfectly isotropic point source is given by ($q_+ = 1/2, q_- = 1/2$).

To solve Eq. (2.1) an infinite number of boundary conditions needs to be satisfied. We need to know $I(x, y, z=0, \Omega)$ for all Ω with either $\cos \theta > 0$ or $\cos \theta < 0$ [23]. For example, if the velocity vector Ω were discretized into 360 angles, the Boltzmann equation (2.1) would represent a set of 360 coupled first-order partial differential equations whose solution is uniquely specified by knowing each of these 360 functions at each point on an infinite open surface. In case of a closed surface, we only need to know the irradiance for either the incoming or outgoing direction relative to the closed surface. This is equivalent to knowing 180 functions of \mathbf{r} at each point on the closed surface. Equivalently, in principle, by successively eliminating higher-order moments, we could replace these 360 first-order differential equations by a single equation of 360th order for the lowest moment, the fluence, $\Phi(\mathbf{r}) \equiv \int d\Omega I(\mathbf{r}, \Omega)$. This equation for $\Phi(\mathbf{r})$ would require the knowledge of 180 constraints with regard to its derivatives at a closed surface. The problem we are faced with in the traditional diffusion approximation is that once we have truncated the order of this differential equation to only second order, the many boundary conditions in the original problem would overdetermine a possible solution for the fluence. In order to obtain a unique solution for the truncated differential equation, we have the arbitrary choice of deciding which of these original 180 boundary conditions the fluence has to satisfy.

III. THE DIFFUSION MODEL

The usual diffusion model is based on the expansion $I_d(\mathbf{r}, \Omega) \approx [\Phi_d(\mathbf{r}) + 3\Omega \cdot \mathbf{J}_d(\mathbf{r})]/4\pi$, and assumes that the most

dominant contribution in $I(\mathbf{r}, \Omega)$ is the energy density or fluence (zeroth velocity moment) defined as $\Phi_d(\mathbf{r}) \equiv \int d\Omega I_d(\mathbf{r}, \Omega)$ followed by the vector flux (current density) $\mathbf{J}_d(\mathbf{r}) \equiv \int d\Omega \Omega I_d(\mathbf{r}, \Omega)$. The diffusion equation is (see Appendix A)

$$(\nabla^2 - \alpha^2)\Phi_d(\mathbf{r}) = (-q/D + 3q_\Delta \partial_z^2/2) \delta(x) \delta(y) \delta(z - z_s), \quad (3.1)$$

where $D \equiv 1/[3(\mu_T - g\mu_s)]$ is the diffusion constant, $\alpha^2 \equiv \mu_a/D$ and $\partial_z \equiv \partial/\partial z$. The source terms consists of the isotropic part $q \equiv q_+ + q_-$ and the anisotropic part $q_\Delta \equiv q_+ - q_-$. The parameter g is the average cosine of the scattering angle $g \equiv \int d\Omega (\Omega \cdot \Omega') p(\Omega \cdot \Omega')$ and has the range $-1 < g < 1$. In essence, the diffusion model approximates the scattering phase function by $p(\Omega \cdot \Omega') \approx [1 + 3g(\Omega \cdot \Omega')]/4\pi$, which is often referred to as the Eddington phase function. This phase function is unreliable for highly forward scattering media as it is positive only for the range $-1/3 < g < 1/3$. In Appendix A, we give the general solutions to Eq. (3.1) for $\Phi_d(\mathbf{r})$ and $\mathbf{J}_d(\mathbf{r})$ containing expansion coefficients that are determined by the particular choice of the boundary condition.

A. Exact boundary conditions

In the presence of an interface, the boundary conditions relate a photon in the direction Ω' to a reflected photon in the direction Ω by a reflection probability $R(\Omega, \Omega')$, which can be modeled as a function of Ω and Ω' [14]. In other words, $I_d(\rho, z=0, \Omega) \Theta(\cos \theta) = \int_- R(\Omega, \Omega') I_d(\rho, z=0, \Omega') d\Omega'$, where the integral \int_- extends over velocity directions with $\cos \theta' < 0$ and $\rho \equiv (x^2 + y^2)^{1/2}$. This relation represents an infinite number of conditions for all values of θ in the range $0 < \theta < \pi/2$. In general, conditions for the moments can be obtained from this relationship by integrating it with respect to $d\Omega$ and $\Omega d\Omega$. The resulting equations have only the trivial solution $\Phi_d(\rho, z=0) = J_{d\rho}(\rho, z=0) = J_{dz}(\rho, z=0) = 0$. This problem is clearly seen for the special case of a nonreflecting interface $R(\Omega, \Omega') = 0$, where the condition requires $I_d(\rho, z=0, \Omega) = [\Phi_d(\rho, z=0) + 3\Omega \cdot \mathbf{J}_d(\rho, z=0)]/(4\pi) = 0$ for all Ω with $0 < \theta < \pi/2$. As this equality has to be true for a continuous set of values for Ω , the only way to fulfill these conditions is $\Phi_d(\rho, z=0) = J_{d\rho}(\rho, z=0) = J_{dz}(\rho, z=0) = 0$. Among these three conditions only $\Phi_d(\rho, z=0) = 0$ and $\partial_z \Phi_d(\mathbf{r}) = 0$ are independent (due to Fick's law as described in Appendix A), but they are unphysical because they imply that there are no photons near the surface $z=0$. Furthermore, both conditions cannot even be imposed simultaneously on Eq. (3.1) as only one boundary condition on a closed surface is required to solve the Helmholtz equation uniquely. In other words, the exact boundary conditions cannot be fulfilled for the diffusion model and we have to resort to approximations. In fact, this conclusion raises a more fundamental question: Is it at all possible to impose the exact boundary conditions on any finite expansion of $I(\mathbf{r}, \Omega)$? We will address this interesting question in Sec. IV, where despite the finiteness of a new expansion of $I(\mathbf{r}, \Omega)$, surprisingly, the exact boundary conditions can be satisfied for special cases.

B. Approximate partial current (PB) and extrapolated (EB) boundary conditions

There are infinitely many approximate boundary conditions that can be imposed on the diffusion equation and only a comparison with the solution of the Boltzmann equation can serve as a yardstick to judge the appropriateness of each particular choice. In Appendix A we discuss various choices and for brevity, we summarize here just the two final expressions. In Sec. V we will discuss their numerical predictions. If there is reflection at the boundary due to an index of refraction mismatch, we can define a reflection coefficient as $r_{11} \equiv -[\int_+ d\Omega \cos \theta I_d(\mathbf{r}, \Omega)] / [\int_- d\Omega \cos \theta I_d(\mathbf{r}, \Omega)]$. The reason for subscript 11 will be clear when we discuss the VHS model in Sec. IV.

In the presence of a reflecting boundary, the partial current boundary condition (PB) is given by $(1-2D\gamma\partial_z)\Phi_{dP}(x, y, z=0)=0$, where $\gamma \equiv (1+r_{11})/(1-r_{11})$ [16–19]. It leads to the solution

$$\begin{aligned} \Phi_{dP}(\mathbf{r}) = & \gamma(q + 3q_\Delta D\partial_z/2) \int_0^\infty d\lambda \lambda J_0(\lambda\rho) \\ & \times \exp[-\alpha_\lambda(z+z_s)] / [\pi(1+2D\gamma\alpha_\lambda)] - (q/D \\ & + 3q_\Delta\partial_z/2) \exp(-\alpha|\mathbf{r}+z_s\mathbf{e}_z|) / (4\pi D|\mathbf{r}+z_s\mathbf{e}_z|) + (q/D \\ & - 3q_\Delta\partial_z/2) \exp(-\alpha|\mathbf{r}-z_s\mathbf{e}_z|) / (4\pi D|\mathbf{r}-z_s\mathbf{e}_z|). \end{aligned} \quad (3.2)$$

The extrapolated boundary condition (EB) involves changing $2D\gamma$ with $2.131D\gamma$ in Eq. (3.2) and the approximation $(1-2.131\gamma D\partial_z)\Phi_{dE}(\mathbf{r}) \approx \Phi_{dE}(x, y, z-2.131\gamma D)=0$. It leads to the solution

$$\begin{aligned} \Phi_{dE}(\mathbf{r}) = & -(q/D + 3q_\Delta\partial_z/2) \exp[-\alpha|\mathbf{r}+(z_s \\ & + 4.262\gamma D)\mathbf{e}_z|] / [4\pi D|\mathbf{r}+(z_s+4.262\gamma D)\mathbf{e}_z|] + (q/D \\ & - 3q_\Delta\partial_z/2) \exp(-\alpha|\mathbf{r}-z_s\mathbf{e}_z|) / (4\pi D|\mathbf{r}-z_s\mathbf{e}_z|) \end{aligned} \quad (3.3)$$

often used [20–22] as an improvement over Eq. (3.2). It should be kept in mind that the derivation [22] of the EB correction factor 2.131 for the position of the extrapolated boundary assumed isotropic scattering ($g=0$), while tissue-like media are highly forward scattering ($g=0.8$ to 0.99). In general, the location of an extrapolated boundary varies for media with different scattering parameters and can only be obtained numerically [14]. As this correction is based on a steady state analysis there is also no evidence that this Milne problem based correction is sufficient for temporal [20] and frequency modulated sources.

The EB approach has an additional problem with regard to the conservation of norm for a source of finite strength. The conservation condition does not exist for the Milne problem as it describes an infinitely extended source. However, for a point source of unit strength, and for $\mu_a=0$ and $r_{11}=0$, the total flux of light coming out from a surface enclosing the medium is $\int d\mathbf{r} \nabla \cdot \mathbf{J}(\mathbf{r}) = -\int dx dy J_z(\rho, z=0) = 1$, reflecting the conservation of the number of particles. If, however, we calculate the flux of light escaping at $z=0$, we obtain $\int dx dy \int_- d\Omega (-\cos \theta) I_{dE}(\rho, z=0, \Omega) = 1.0324$. The reason for this violation of norm conservation is that, due to the extrapolation assumption, there is an (unphysical) flux that

enters the medium with strength $\int dx dy \int_+ d\Omega \cos \theta I_{dE}(\rho, z=0, \Omega) = 0.0324$. The correction of $2.131D$ assumes implicitly a finite reflection at the boundary (even for an index matched medium) and therefore (unphysically) overestimates the output flux to guarantee that the net flux can fulfill $\int dx dy \int d\Omega \cos \theta I_{dE}(\rho, z=0, \Omega) = 1$ at $z=0$.

IV. THE VELOCITY HALF-SPHERE (VHS) MODEL

In Ref. [23] we introduced the velocity half-sphere model where the total irradiance was separated into two portions $I(\mathbf{r}, \Omega) \equiv I_+(\mathbf{r}, \Omega)\Theta(\cos \theta) + I_-(\mathbf{r}, \Omega)\Theta(-\cos \theta)$. We denote the irradiance in the range $0 \leq \theta < \pi/2$ by $I_+(\mathbf{r}, \Omega)$ and for $\pi/2 \leq \theta < \pi$ by $I_-(\mathbf{r}, \Omega)$. Consistent with this separation and the doubling of the resulting phase-space variables, this approach leads to four (instead of two) velocity moments $\Phi_\pm(\mathbf{r}) \equiv \int_\pm d\Omega I(\mathbf{r}, \Omega)$ and $\mathbf{J}_\pm(\mathbf{r}) \equiv \int_\pm d\Omega \Omega I(\mathbf{r}, \Omega)$. If we assume that the half-sphere irradiances $I_+(\mathbf{r}, \Omega)$ and $I_-(\mathbf{r}, \Omega)$ are linear in Ω , we obtain the expansions

$$\begin{aligned} I_\pm(\mathbf{r}, \Omega) \approx & [2\Phi_\pm(\mathbf{r}) \mp 3J_{\pm z}(\mathbf{r})] / \pi + 3\Omega \cdot \{\mathbf{J}_\pm(\mathbf{r}) \\ & + [3J_{\pm z}(\mathbf{r}) \mp 2\Phi_\pm(\mathbf{r})]\mathbf{e}_z\} / (2\pi). \end{aligned} \quad (4.1)$$

Note that this expansion is different from a double- P_L approximation, which is based on half-range Legendre polynomials [2]. The double- P_L approximation is very complicated in the presence of transverse effects and the physical interpretation of various moments is not straightforward. Both of these problems do not exist for the above expansion, which is based on the assumption that $I_\pm(\mathbf{r}, \Omega)$ are linear in Ω . Let us now use the expansion (4.1) to derive the corresponding equations for the four moments $J_\pm(\mathbf{r})$ and $\Phi_\pm(\mathbf{r})$ from the Boltzmann equation. It turns out that the set of moments defined as $\Phi(\mathbf{r}) \equiv \Phi_+(\mathbf{r}) + \Phi_-(\mathbf{r})$, $\Phi\Delta(\mathbf{r}) \equiv \Phi_+(\mathbf{r}) - \Phi_-(\mathbf{r})$, $\mathbf{J}(\mathbf{r}) \equiv \mathbf{J}_+(\mathbf{r}) + \mathbf{J}_-(\mathbf{r})$, and $\mathbf{J}\Delta(\mathbf{r}) \equiv \mathbf{J}_+(\mathbf{r}) - \mathbf{J}_-(\mathbf{r})$ leads to simpler equations. Furthermore, $\Phi(\mathbf{r})$ and $\mathbf{J}(\mathbf{r})$ provide a direct comparison with the usual diffusion model.

The equations for $\mathbf{J}(\mathbf{r})$ and $\mathbf{J}\Delta(\mathbf{r})$ can be obtained by inserting the expansion Eq. (4.1) into the transport equation (2.1) with the Eddington phase function. The resulting equations for $I_\pm(\mathbf{r}, \Omega)$ are

$$\begin{aligned} (\Omega \cdot \nabla + \mu_T) I_\pm(\mathbf{r}, \Omega) = & \mu_s [\Phi(\mathbf{r}) + 3g\Omega \cdot \mathbf{J}(\mathbf{r})] / (4\pi) \\ & + q_\pm \delta(x) \delta(y) \delta(z-z_s) / (2\pi). \end{aligned} \quad (4.2)$$

The right hand side can be obtained using the identity $\Omega \cdot \Omega' = \cos \theta \cos \theta' + \sin \theta \sin \theta' \cos(\phi - \phi')$. Integrating Eq. (4.2) over the velocity half-sphere $\int_\pm d\Omega$ leads to $\nabla \cdot \mathbf{J}_\pm(\mathbf{r}) = -\mu_T \Phi_\pm(\mathbf{r}) + \mu_s [\Phi(\mathbf{r}) / 2 \pm 3gJ_z(\mathbf{r}) / 4] + q(\mathbf{r}) / 2$. If we add and subtract these two equations from each other we obtain the two scalar equations

$$\nabla \cdot \mathbf{J}(\mathbf{r}) = -\mu_a \Phi(\mathbf{r}) + q \delta(x) \delta(y) \delta(z-z_s) \quad (4.3a)$$

$$\nabla \cdot \mathbf{J}\Delta(\mathbf{r}) = -\mu_T \Phi\Delta(\mathbf{r}) + 3g\mu_s J_z(\mathbf{r}) / 2 + q_\Delta \delta(x) \delta(y) \delta(z-z_s). \quad (4.3b)$$

The derivation of the corresponding two vector equations for Φ and $\Phi\Delta$ is more complicated and a careful inspection

of the terms on the left-hand side of Eq. (4.2) shows there are odd and even power terms of $\sin \theta$ and $\cos \theta$. These terms are independent of each other as one can see by integrating Eq. (4.2) with respect to $\int_{\pm} d\Omega \Omega P_n(\cos \theta)$, where P_n is the fifth or higher odd-order Legendre polynomial [23]. The resulting equations are given by

$$\begin{aligned} \nabla[2\Phi_{\pm}(\mathbf{r}) \mp 3J_{\pm z}(\mathbf{r})] &= -3\mu_T \mathbf{J}_{\pm}(\mathbf{r}) \\ &+ [3J_{\pm z}(\mathbf{r}) \mp 2\Phi_{\pm}(\mathbf{r})] \mathbf{e}_z / 2 \\ &+ 3\mu_s g \mathbf{J}(\mathbf{r}). \end{aligned} \quad (4.4)$$

By subtracting and adding these two equations from each other we obtain $J_{\Delta z}(\mathbf{r}) = \Phi(\mathbf{r})/2 - \partial_z Y(\mathbf{r})/(6\mu_T)$, where $Y(\mathbf{r}) \equiv 2\Phi_{\Delta}(\mathbf{r}) - 3J_z(\mathbf{r})$. Using these expressions we can write equations for \mathbf{J} and \mathbf{J}_{Δ} as

$$\mathbf{J}(\mathbf{r}) = -D \nabla [\Phi(\mathbf{r}) + \partial_z Y(\mathbf{r})/\mu_T] + 3D\mu_T Y(\mathbf{r}) \mathbf{e}_z \quad (4.5a)$$

$$\mathbf{J}_{\Delta}(\mathbf{r}) = -2 \nabla Y(\mathbf{r})/(3\mu_T) + [\partial_z Y(\mathbf{r})/(2\mu_T) + \Phi(\mathbf{r})/2] \mathbf{e}_z. \quad (4.5b)$$

Note that the first equation is a generalized version of Fick's law. It contains J_z also on the right hand side and thus should be seen as a differential equation for J_z . Equation (4.5b), however, represents \mathbf{J}_{Δ} in terms of Φ , Φ_{Δ} , and J_z . By substituting $\mathbf{J}_{\Delta}(\mathbf{r})$ and $J_z(\mathbf{r})$ from Eqs. (4.5) into (4.3b) we obtain

$$(\nabla^2 - 3\mu_T^2)Y(\mathbf{r}) = -3\mu_T q_{\Delta} \delta(x) \delta(y) \delta(z - z_s)/2. \quad (4.6)$$

Equation (4.6) is crucial as its solution $Y(\mathbf{r})$ is related to the difference between $\Phi_{\Delta}(\mathbf{r})$ and $J_z(\mathbf{r})$. The source term on the right hand side is zero if the source in the Boltzmann equation is isotropic. The main difference between diffusion theory and the VHS model is the quantity $Y(\mathbf{r})$. The traditional diffusion theory predicts a vanishing $Y(\mathbf{r})$, because $2\Phi_{\Delta}(\mathbf{r}) = 3J_z(\mathbf{r})$ and thus it is an important measure. Applying the gradient operator ∇ on Eq. (4.5a) and substituting in Eq. (4.3a) we also arrive at the usual diffusion equation given by

$$(\nabla^2 - \alpha^2)\Phi(\mathbf{r}) = (-q/D + 3q_{\Delta} \partial_z^2/2) \delta(x) \delta(y) \delta(z - z_s). \quad (4.7)$$

As shown in Ref. [23] the VHS model is more accurate in infinite media than the diffusion model for anisotropic sources due to the doubling of the phase space variables. In order to focus on how the VHS model can also describe physical interfaces more accurately, we purposely restrict our discussion here to the special case of sources, for which both theories predict identical fluence for an infinite medium.

Note that Eqs. (4.6) and (4.7) form a set of two second-order partial differential equations, which can be solved uniquely if $\Phi(\mathbf{r})$ and $Y(\mathbf{r})$ are specified on a boundary. The half fluxes $\mathbf{J}_{\pm}(\mathbf{r})$ and half fluences $\Phi_{\pm}(\mathbf{r})$ are related to $\Phi(\mathbf{r})$ and $Y(\mathbf{r})$ through the relations (4.5) and the definition of $Y(\mathbf{r})$, i.e., $\Phi_{\Delta}(\mathbf{r}) = 3J_z(\mathbf{r})/2 + Y(\mathbf{r})/2$. Using these relations and some rearrangements, the following expressions for the half fluxes and fluences are obtained:

$$\begin{aligned} J_{\pm z}(\mathbf{r}) &= (\pm 1 - 2D\partial_z)\Phi(\mathbf{r})/4 - [6D(\partial_z^2 \\ &- 3\mu_T^2) \pm \partial_z]Y(\mathbf{r})/(12\mu_T), \end{aligned} \quad (4.8a)$$

$$J_{\pm \rho}(\mathbf{r}) = -D\partial_{\rho} \{\Phi(\mathbf{r}) + [\partial_z \pm 2/(3D)]Y(\mathbf{r})/\mu_T\}/2, \quad (4.8b)$$

$$\begin{aligned} \Phi_{\pm}(\mathbf{r}) &= (2 \mp 3D\partial_z)\Phi(\mathbf{r})/4 \mp [3D(\partial_z^2 - 3\mu_T^2) + 1]Y(\mathbf{r})/(4\mu_T) \\ &= \pm 3J_{\pm z}(\mathbf{r})/2 + [\Phi(\mathbf{r}) + (\partial_z \pm 2\mu_T)Y(\mathbf{r})/\mu_T]/8. \end{aligned} \quad (4.8c)$$

Generally, either $I_+(\mathbf{r}, \Omega)$ or $I_-(\mathbf{r}, \Omega)$ is given as a boundary condition on a closed surface, thus at least three of the above six quantities are known at an interface or a boundary permitting a solution of Eqs. (4.6) and (4.7).

A. General solution for the VHS model

The general solution for $\Phi(\mathbf{r})$ and $Y(\mathbf{r})$ can be obtained using the Hankel transformations

$$\begin{aligned} \Phi(\mathbf{r}) &= \int_0^{\infty} d\lambda A_{\lambda} \lambda J_0(\lambda \rho) \exp(-\alpha_{\lambda} z)/(4\pi D \alpha_{\lambda}) \\ &+ \int_0^{\infty} d\lambda \lambda J_0(\lambda \rho) (q/D - 3q_{\Delta} \partial_z^2/2) \exp(-\alpha_{\lambda} |z \\ &- z_s|)/(4\pi \alpha_{\lambda}), \end{aligned} \quad (4.9a)$$

$$\begin{aligned} Y(\mathbf{r}) &= \int_0^{\infty} d\lambda B_{\lambda} \lambda J_0(\lambda \rho) \exp(-\mu_{\lambda} z)/(2\pi) \\ &+ 3q_{\Delta} \mu_T \int_0^{\infty} d\lambda \lambda J_0(\lambda \rho) \exp(-\mu_{\lambda} |z - z_s|)/(8\pi \mu_{\lambda}), \end{aligned} \quad (4.9b)$$

where $J_n(\dots)$ is the n th order Bessel function and $\mu_{\lambda} \equiv \sqrt{(\lambda^2 + 3\mu_T^2)}$. The corresponding solution for the transformed half-fluxes and half-fluences are

$$\begin{aligned} \Phi_{\pm}(\mathbf{r}) &= \int_0^{\infty} d\lambda \lambda J_0(\lambda \rho) \{A_{\lambda} (2 \pm 3\alpha_{\lambda}) \exp(-\alpha_{\lambda} z)/(32\pi D \alpha_{\lambda}) \\ &+ q(2 \pm 3D\alpha_{\lambda} \text{Si}(z)) \exp(-\alpha_{\lambda} |z - z_s|)/(32\pi D \alpha_{\lambda}) \\ &+ 3q_{\Delta} [2\text{Si}(z) \pm 3D\alpha_{\lambda}] \exp(-\alpha_{\lambda} |z - z_s|)/(32\pi) \\ &\pm (-3D\lambda^2 + \mu_T) B_{\lambda} \exp(-\mu_{\lambda} z)/(8\pi D \mu_T) \\ &\mp 3q_{\Delta} (3D\lambda^2 + 1) \exp(-\mu_{\lambda} |z - z_s|)/(32\pi \mu_{\lambda}) \} \end{aligned} \quad (4.10a)$$

$$\begin{aligned} J_{\pm z}(\mathbf{r}) &= \int_0^{\infty} d\lambda \lambda J_0(\lambda \rho) \{A_{\lambda} (\pm 1 + 2D\alpha_{\lambda}) \exp(-\alpha_{\lambda} z)/(\\ &(16\pi D \alpha_{\lambda}) + q[\pm 1 + 2D\alpha_{\lambda} \text{Si}(z)] \exp(-\alpha_{\lambda} |z \\ &- z_s|)/(16\pi D \alpha_{\lambda}) + 3q_{\Delta} (\pm \text{Si}(z) + 2D\alpha_{\lambda}) \exp(-\alpha_{\lambda} |z \\ &- z_s|)/(32\pi) + (-D\lambda^2 \pm \mu_{\lambda}/6) B_{\lambda} \exp(-\mu_{\lambda} z)/(\\ &(4\pi D \mu_T) + q_{\Delta} [-6D\lambda^2 \pm \mu_{\lambda} \text{Si}(z)] \exp(-\mu_{\lambda} |z \\ &- z_s|)/(32\pi \mu_{\lambda}) \}, \end{aligned} \quad (4.10b)$$

$$\begin{aligned}
J_{\pm\rho}(\mathbf{r}) = & \int_0^\infty d\lambda \lambda^2 J_1(\lambda\rho) (\{A_\lambda \exp(-\alpha_\lambda z) + [q \\
& + 3q_\Delta D\alpha_\lambda \text{Si}(z)/2] \exp(-\alpha_\lambda |z - z_s|)\} / (8\pi\alpha_\lambda) \\
& + (-D\mu_\lambda \pm 2/3)B_\lambda \exp(-\mu_\lambda z) / (4\pi\mu_T) \\
& + 3Dq_\Delta [-3D\mu_\lambda \text{Si}(z) \pm 2] \\
& \times \exp(-\mu_\lambda |z - z_s|) / (16\pi\mu_\lambda)), \quad (4.10c)
\end{aligned}$$

where $\text{Si}(z) \equiv [2\Theta(z - z_s) - 1]$ is the sign function. In contrast to the solution of the diffusion theory, we have double the amount of parameters available to find the solution for the appropriate boundary condition. There are two sets of expansion coefficients A_λ and B_λ which can be obtained from two boundary conditions at the interface $z=0$. Among the six half-sphere variables given in Eq. (4.8) if any two are known at the interface, then we can find A_λ and B_λ uniquely. This additional degree of freedom suggests that the VHS model should be much better suited for describing the light distribution close to physical interfaces but it comes with a trade off that double the number of boundary conditions are required as compared to the usual diffusion model.

B. Exact boundary conditions for VHS model

The exact boundary conditions are given by $I_+(\rho, z=0, \Omega) = \int_- R(\Omega, \Omega') I_-(\rho, z=0, \Omega') d\Omega'$, which can be further integrated to give three general relations of the type $J_{+z}(\rho, z=0) = -r_{11}J_{-z}(\rho, z=0) + r_{12}\Phi_-(\rho, z=0) + r_{13}J_{-\rho}(\rho, z=0)$, $\Phi_+(\rho, z=0) = -r_{21}J_{-z}(\rho, z=0) + r_{22}\Phi_-(\rho, z=0) + r_{23}J_{-\rho}(\rho, z=0)$ and $J_{+\rho}(\rho, z=0) = -r_{31}J_{-z}(\rho, z=0) + r_{32}\Phi_-(\rho, z=0) + r_{33}J_{-\rho}(\rho, z=0)$. We now have three conditions and two unknown sets of coefficients A_λ and B_λ in the general solutions (4.10). Thus the problem is still over determined, however, there are special cases for which one of the three boundary conditions is redundant. In those situations we can impose the boundary conditions exactly. For example, when $R(\Omega, \Omega')=0$, apparently the boundary conditions are $J_{+z}(\rho, z=0) = J_{+\rho}(\rho, z=0) = \Phi_+(\rho, z=0) = 0$. If the medium scatters isotropically ($g=0$), the condition $J_{+\rho}(\rho, z=0) = 0$ is redundant because it follows directly from Eq. (4.8c) if $\Phi_+(\rho, z=0) = 0$ and $J_{+z}(\rho, z=0) = 0$. Thus only two conditions are required permitting a unique determination of the coefficients A_λ and B_λ . We denote these exact boundary condition solutions with a superscript 0, i.e., $\Phi^{(0)}(\mathbf{r})$, and $Y^{(0)}(\mathbf{r})$, and the coefficients for an isotropic source are given by

$$\begin{aligned}
A_\lambda^{(0)} = & -(\mu_\lambda + \alpha_\lambda) \exp(-\alpha_\lambda z_s) / (\mu_\lambda - \alpha_\lambda) \\
= & -[1 + 2\alpha_\lambda(\mu_\lambda + \alpha_\lambda) / (3\mu_T^2 - \alpha^2)] \exp(-\alpha_\lambda z_s), \quad (4.11a)
\end{aligned}$$

$$B_\lambda^{(0)} = -3\mu_T^2 \exp(-\alpha_\lambda z_s) / [(\mu_\lambda - \alpha_\lambda)(\mu_\lambda - 2\mu_T)]. \quad (4.11b)$$

The integral relations in Eq. (4.9) determine $\Phi(\mathbf{r})$ and $Y(\mathbf{r})$, and the half-moments can be obtained from Eq. (4.10). The expression for the fluence can be further simplified to

$$\begin{aligned}
\Phi^{(0)}(\mathbf{r}) = & - \int_0^\infty d\lambda \lambda J_0(\lambda\rho) \exp[-\alpha_\lambda(z + z_s)] (\mu_\lambda \\
& + \alpha_\lambda) / [2\pi D(3\mu_T^2 - \alpha^2)] - \exp(-\alpha|\mathbf{r} \\
& + z_s \mathbf{e}_z|) / (4\pi D|\mathbf{r} + z_s \mathbf{e}_z|) + \exp(-\alpha|\mathbf{r} - z_s \mathbf{e}_z|) / (4\pi D|\mathbf{r} \\
& - z_s \mathbf{e}_z|). \quad (4.12)
\end{aligned}$$

Note that in spite of the finitude of the expansion of $I(\mathbf{r}, \Omega)$, we have successfully imposed the exact boundary conditions of the Boltzmann equations. This is an additional advantage of the VHS model over the usual expansion in terms of full range spherical harmonics where this cannot be achieved. Unfortunately, the above result predicts an unphysical negative fluence at the boundary $z=0$ for the special case when $3\mu_T > \alpha$. Interestingly, the reason for this disappointing result is the boundary condition $\Phi_+(\rho, z=0) = 0$, which as we show in Appendix B, can be associated with a discontinuity at $z=0$. Note that r_{22} is the ratio of densities $\Phi_+(\rho, z=0) / \Phi_-(\rho, z=0)$ when r_{21} and r_{23} are zero. Unlike r_{11} , even for an index-matched medium we do not expect r_{22} to be zero at the interface between two media with different scattering properties. Unfortunately, the exact functional form of $R(\Omega, \Omega')$ is not known and only approximate forms can be assumed, for example, using Fresnel relations which only considers flux information and not the irradiance $I(\mathbf{r}, \Omega)$.

Nonetheless, the problem of discontinuity in $\Phi_+(\rho, z=0)$ can be avoided by imposing the boundary condition at $z=0^+$ which is slightly inside the medium. This problem does not arise for the diffusion model because it does not treat half-fluences $\Phi_\pm(\mathbf{r})$. However, if we evaluate the half-fluence for the special case of an isotropic source ($q_\pm = 1/2$), $\mu_a = 0$ and a nonreflecting interface at $z=0$, the diffusion model predicts $2\pi \int \rho d\rho \int d\Omega I_d(\rho, z=0, \Omega) = 0.25$ and not zero. If we use this value as a boundary condition for the VHS model, we obtain exactly the same result as the diffusion model. Thus if the exact boundary value for $\Phi_+(\rho, z=0^+)$ is known, the VHS model could provide significant improvements over the diffusion model. Unfortunately a limitation of the VHS model is that this value may not be known in advance and has to be obtained from prior experimental measurements slightly inside the surface $z=0$ or from the Monte Carlo (MC) simulations. The half-fluence can be measured using different opening angles of a detector. For example, if a point detector is oriented along the negative z direction and has an opening angle of α , then the light measured is $\int_0^\alpha d(\cos \theta) \int_0^{2\pi} d\phi \cos \theta I_+(\mathbf{r}, \Omega) = 2\Phi_+(\mathbf{r})(\sin^2 \alpha + \cos^3 \alpha - 1) + J_{+z}(\mathbf{r})(4 - 3\sin^2 \alpha - 4\cos^3 \alpha)$, where we have used expansion (4.1) for $I_+(\mathbf{r}, \Omega)$. Using detectors with two different opening angles both $J_{+z}(\mathbf{r})$ and $\Phi_+(\mathbf{r})$ can be measured at every location.

C. Approximate boundary conditions for VHS model

The functional form of $R(\Omega, \Omega')$ is in general unknown and has to be obtained experimentally or using the fundamental Maxwell equations.

Specular reflection. A specular reflection occurs when the angle between incident ($\Omega' - \pi$) and reflected (Ω) light is 2θ

for $\theta' - \pi < \theta_c$, otherwise the reflection is zero. Thus for $\theta' - \pi < \theta_c$, $R(\Omega, \Omega') = r(\cos \theta, n, n_0) \delta(-\cos \theta' - \cos \theta) \delta(\phi' - \phi)$, where n and n_0 are the refractive indices of the regions $z > 0$ and $z < 0$, respectively, and $r(\cos \theta, n, n_0)$ is the Fresnel coefficient for unpolarized light reflecting from an interface [24]. After integrating over Ω' the boundary condition reduces to

$$\begin{aligned} I_+(\rho, z=0, \Omega) &= r(\cos \theta, n, n_0)[2(2 - 3 \cos \theta)\Phi_-(\rho, z=0) \\ &+ 6(1 - 2 \cos \theta)J_{-z}(\rho, z=0) + 3 \cos \phi J_{-x}(\rho, z=0) \\ &+ 3 \sin \phi J_{-y}(\rho, z=0)]/(2\pi), \quad \text{for } \theta < \theta_c, \\ I_+(\rho, z=0, \Omega) &= 0, \quad \text{for } \theta \geq \theta_c. \end{aligned} \quad (4.13)$$

Further integration with respect to $\int_+ d\Omega$ and $\int_+ \Omega d\Omega$ leads to the first set of boundary conditions $J_{+z}(\rho, z=0) = -r_{11}J_{-z}(\rho, z=0) + r_{12}\Phi_-(\rho, z=0)$ and $\Phi_+(\rho, z=0) = -r_{21}J_{-z}(\rho, z=0) + r_{22}\Phi_-(\rho, z=0)$.

If the interface is a rough surface such that the incident light can be uniformly reflected in all directions we can model this type of reflection as $R(\Omega, \Omega') = p/2\pi$, where p is the fraction of light which is reflected. In these cases we have $I_+(\rho, z=0, \Omega) = p\Phi_-(\rho, z=0)/2\pi$ and the second set of boundary conditions is $\Phi_+(\rho, z=0) = p\Phi_-(\rho, z=0)$ and $J_{+z}(\rho, z=0) = p\Phi_-(\rho, z=0)/2$. These two sets of boundary conditions above cannot be taken accurately into account in the diffusion model. In fact, the diffusion model is always solved for the boundary condition $J_{+z}(\rho, z=0) = -r_{11}J_{-z}(\rho, z=0)$. For the VHS model, different solutions are possible depending on the type of reflection from the interface.

In the following, we provide solution to the VHS model by assuming that we know $r_{11} = -J_{+z}(\rho, z=0)/J_{-z}(\rho, z=0)$ and $\Phi_+(\rho, z=0^+)$. The former boundary condition which, approximately represent a specularly reflecting boundary, provides a fair comparison between the VHS and diffusion model. The second condition is fairly general and applicable irrespective of the type of reflection at the interface. Note that we have chosen to impose the boundary condition for half-fluence slightly inside the medium $z=0^+$ and not at $z=0$ due to the discontinuity problem as discussed in the previous section and in Appendix B. With these boundary conditions and the coefficients A_λ and B_λ are

$$\begin{aligned} A_\lambda &= \{-[X_1(1 - 2D\gamma\alpha_\lambda) - X_2(2 - 3D\alpha_\lambda)](q - 3q_\Delta D\alpha_\lambda/2) \\ &\times \exp(-\alpha_\lambda z_s) - 8D\alpha_\lambda f_\lambda X_2 + q_\Delta D\alpha_\lambda X_1 \\ &\times \exp(-\mu_\lambda z_s)\}/[X_1(1 + 2D\gamma\alpha_\lambda) - X_2(2 + 3D\alpha_\lambda)], \end{aligned} \quad (4.14a)$$

$$\begin{aligned} B_\lambda &= \{(3 - 4\gamma)(q - 3q_\Delta D\alpha_\lambda/2)\exp(-\alpha_\lambda z_s) + 4f_\lambda(1 + 2D\gamma\alpha_\lambda) \\ &- q_\Delta[3\mu_T(1 + 2D\gamma\alpha_\lambda) + \mu_\lambda(2 + 3D\alpha_\lambda) - 3D\lambda^2(3 \\ &- 4\gamma)]\exp(-\mu_\lambda z_s)/(4\mu_\lambda)\}/[X_1(1 + 2D\gamma\alpha_\lambda) - X_2(2 \\ &+ 3D\alpha_\lambda)], \end{aligned} \quad (4.14b)$$

where $X_1 \equiv (-3D\lambda^2/\mu_T)$, $X_2 \equiv \mu_\lambda/(3\mu_T) - 2D\gamma\lambda^2/\mu_T$ and $f_\lambda \equiv 2\pi\int_0^\infty \rho d\rho J_0(\lambda\rho)\Phi_+(\rho, z=0^+)$. These expressions have a complicated dependence on λ and the solutions for $\Phi(\mathbf{r})$ and

$Y(\mathbf{r})$ have to be obtained by numerical integration. We discuss next the special case for which the variables are integrated over the entire xy plane, corresponding to taking the limit $\lambda=0$. This simplifies Eq. (4.14) to

$$\begin{aligned} A_0 &= \{-[(1 - 2D\gamma\alpha) - (2 - 3D\alpha)/\sqrt{3}](q - 3q_\Delta D\alpha/2) \\ &\times \exp(-\alpha z_s) - 8D\alpha f_0/\sqrt{3} + q_\Delta D\alpha \exp(-\sqrt{3}\mu_T z_s)\}/[(1 \\ &+ 2D\gamma\alpha) - (2 + 3D\alpha)/\sqrt{3}], \end{aligned} \quad (4.15a)$$

$$\begin{aligned} B_0 &= \{(3 - 4\gamma)(q - 3q_\Delta D\alpha/2)\exp(-\alpha z_s) + 4f_0(1 + 2D\gamma\alpha) \\ &- q_\Delta[\sqrt{3}(1 + 2D\gamma\alpha) + (2 + 3D\alpha)]\exp(-\sqrt{3}\mu_T z_s)/4\}/[(1 \\ &+ 2D\gamma\alpha) - (2 + 3D\alpha)/\sqrt{3}]. \end{aligned} \quad (4.15b)$$

The integrated half-fluxes denoted by $F_\pm(z) \equiv 2\pi\int_0^\infty J_{\pm z}(\mathbf{r})\rho d\rho$ are given by

$$\begin{aligned} F_\pm(z) &= A_0(\pm 1 + 2D\alpha)\exp(-\alpha z)/(8D\alpha) + q[\pm 1 \\ &+ 2D\alpha \text{Si}(z)]\exp(-\alpha|z - z_s|)/(8D\alpha) + 3q_\Delta[\pm \text{Si}(z) \\ &+ 2D\alpha]\exp(-\alpha|z - z_s|)/16 \pm \sqrt{3}B_\lambda \\ &\times \exp(-\mu_\lambda z)/12 \pm q_\Delta \text{Si}(z)\exp(-\sqrt{3}\mu_T|z - z_s|)/16. \end{aligned} \quad (4.16)$$

V. NUMERICAL RESULTS AND COMPARISON WITH MONTE CARLO SIMULATIONS

We have performed numerical simulations for various parameters to compare the traditional PB and EB diffusion theory with the VHS model. The MC simulation, represents the exact solution to the radiative transfer equation (2.1) involving up to 10^8 photons, each of which performed a random walk with a random distance l distributed according to $P(l) = \exp(-\mu_s l)/\mu_s$ and with a random scattering angle Ω distributed according to the scattering phase function $P_{\text{HG}}(\Omega \cdot \Omega') = (1 - g^2)/[4\pi\{1 + g^2 - 2g\Omega\Omega'\}^{2/3}]$. The Boltzmann half-fluxes, denoted by $\mathbf{J}_{\pm B}(\mathbf{r}, t)$, are time dependent and were obtained for a pulsed light source that emitted photons at time $t=0$. In order to obtain the corresponding steady state fluxes from a time-dependent simulation, the resulting photon flux was integrated over a sufficiently large time T according to $\mathbf{J}_{\pm B}(\mathbf{r}) = \int_0^T d\tau \mathbf{J}_{\pm B}(\mathbf{r}, T - \tau)$. For a fair comparison with the extrapolated correction of 2.131 [see Eq. (3.3)], which is derived in the absence of transverse effects, we compute the total z component of the net flux crossing the xy plane at $z=0$, i.e., $F_{\pm B}(z) \equiv 2\pi\int_0^\infty \rho d\rho \int_{-d\Omega} d\Omega \cos \theta I_d(\mathbf{r}, \Omega)$ for the PB and EB conditions. In the numerical analysis below we measure the length in units of μ_s^{-1} and set the speed of light $c=1$.

Let us start the discussion with the case most frequently studied in the literature characterized by an isotropic source, (corresponding to $q_+ = q_- = 1/2$) and no reflection at the boundary $z=0$ and vanishing absorption. The simulations show a difference between the PB solution and the MC simu-

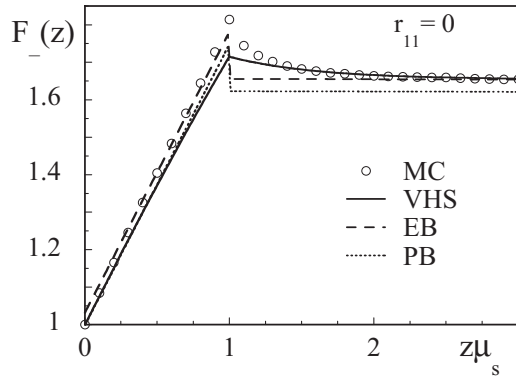


FIG. 1. The integrated flux along the negative z direction for VHS, PB, and EB solutions, compared with the MC simulation for a perfectly index-matched interface. The medium scatters isotropically $g=0$ and without absorption $\mu_a=0$. The anisotropic source ($q_+=1$, $q_-=0$) is located at $z\mu_s=1$. For the VHS model the additional boundary condition is $f_0=0.295$.

lations even at large distances. The EB solution, however, is in good agreement with the MC simulation, because the extrapolated correction of 2.131 is obtained [2] specifically for a medium with $r_{11}=0$, $\mu_a=0$, and $g=0$. Unlike the diffusion theory, the VHS model requires an additional boundary condition for $\Phi_+(\rho, z=0^+)$. This value determines the integrated half-fluence, defined as

$$f_0 \equiv 2\pi \int_0^\infty \rho d\rho \Phi_+(\rho, z=0^+). \quad (5.1)$$

Since this value is not known in advance, we used MC predictions of half-fluence, $2\pi \int_0^\infty \rho d\rho \Phi_+(\mathbf{r})$, to estimate f_0 . To obtain the MC value for half-fluence we set the detector opening angles at $\pi/2$ and $\pi/3$ and both integrated half-flux $2\pi \int_0^\infty \rho d\rho J_{+z}(\mathbf{r})$ and half-fluence were measured. Based on the MC data for half-fluence in the region 0 to $0.5\mu_s$ different values were tried for f_0 to find a suitable fit. It should be noted that we are using the exact data to find an approximate value of $\Phi_+(\mathbf{r})$ based on the expansion (4.1). For the PB model this quantity can be obtained from the diffusive irradiance via $2\pi \int_0^\infty \rho d\rho \int_{-d}^d \Omega I_d(z=0, \rho, \Omega) = 0.25$ (in units of number of photons per unit length), whereas the EB predicts 0.2664. If we choose the boundary condition $f_0=0.258$ for VHS, we find excellent agreement between EB, VHS, and MC solutions. This value was obtained from MC simulations for integrated half-fluence at $z=0.11\mu_s$. At the boundary the MC, VHS, and PB solutions predict the net flux crossing the interface $z=0$ as unity as a result of the conservation condition whereas the EB solution predicts a value 1.0324. We discuss next the result for the same medium with an anisotropic source for which the improvement of the VHS approach over the EB or PB diffusion approach is more significant.

In Fig. 1 we graph the net flux in the negative z direction for a nonabsorbing ($\mu_a=0$) and isotropic scattering ($g=0$) medium without any specular reflection ($r_{11}=0$) at the boundary. The anisotropic source ($q_+=1$, $q_-=0$) is located at $z\mu_s=1$ and emits the light into the positive z direction. Here

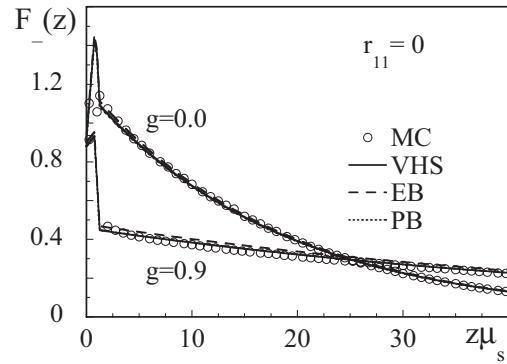


FIG. 2. The integrated flux in the negative z direction for the VHS, PB, and EB models, compared with the MC simulations for a medium with zero reflection $r_{11}=0$ and absorption $\mu_a=0.001\mu_s$ and $f_0=0.23$. The isotropic source ($q_+=1/2$, $q_-=1/2$) is located at $z\mu_s=1$.

and in all the following graphs, we compare the PB (dotted line), the EB (dashed lines), and the VHS theory (continuous line) with the Monte Carlo data (circles). The VHS data were obtained for the boundary condition $f_0=0.295$, a value different from 0.125 as predicted by the PB diffusion model. For small values of z the consequences from the norm conservation problem for EB are evident. In the region $z\mu_s > 1$ we note a significant difference between the MC and PB solution. This difference remains the same even for $z \rightarrow \infty$ as the medium is lossless. The graph for EB shows the improvement due to the correction factor of 2.131 for large z . This agreement between the EB and MC data is not surprising because we examine xy plane integrated quantities where transverse effects are averaged out. However, any measurement using small finite size detectors could reduce the range of validity of the EB solution. The effect of the source anisotropy is seen near the source where the VHS model can predict the smooth exponential decrease to the asymptotic value more reliably than any diffusion model.

Next, let us compare the three solutions in the presence of small absorption $\mu_a=0.001\mu_s$ (similar to a tissuelike medium) on a larger spatial scale. From now on we will use an isotropic source ($q_+=1/2$, $q_-=1/2$). Figure 2 shows the integrated flux for isotropic ($g=0$) as well as highly forward ($g=0.9$) scattering media and zero reflection ($r_{11}=0$). For the larger value of g we replaced the Eddington phase function by the δ -Eddington phase function [10] in the VHS model. This amounts essentially to replacing μ_s by $\mu_s(1-g^2)$ and g by $g/(1+g)$. Such a correction does not make any difference for the two diffusion models. All three approaches agree very well with the MC data. The agreement for $g=0$ deteriorates slightly with increasing anisotropy. While the PB and VHS model remain in good agreement with the MC simulations, the EB data consistently overestimate the MC predictions. This is expected as the correction factor 2.131 was obtained for the case of $g=0$.

Let us now examine the impact of a specular reflection from a mirror at the interface at $z=0$. As introduced in Sec. III, the amount of reflection is determined by the parameter r_{11} , which for simplicity was chosen to be independent of the incoming angle. However, the angles of reflection and inci-

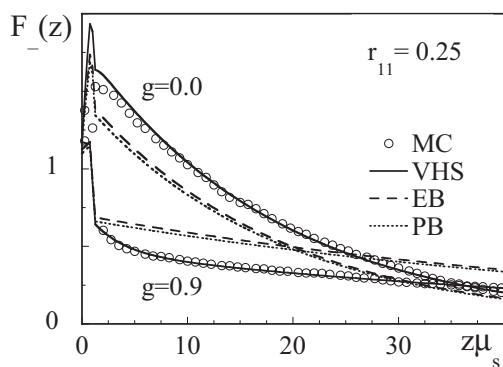


FIG. 3. The impact of a reflecting interface at $z=0$, $r_{11}=0.25$. Total flux in the negative z direction for the VHS, PB, and EB models, compared with the MC simulation. For the VHS model we chose $f_0=0.9$ ($g=0$) and $f_0=0.73$ ($g=0.9$). (Same source and medium parameters as in Fig. 2.)

dence was always set to be equal. In Fig. 3 the reflection coefficient at the interface is $r_{11}=25\%$. In the $g=0$ case both PB and EB underestimate the net flux, whereas for $g=0.9$, the two diffusion theories overestimate it significantly. In both case the VHS model is in good agreement with the MC data.

In Fig. 4 we examine a larger index of refraction mismatch with 50% reflection ($r_{11}=0.5$). While the same conclusions hold, the diffusion theories seem to be even less reliable for these high reflecting interfaces whereas the VHS model is sufficiently accurate except in regions close to the source. In this particular region the VHS model could be improved further [11,12] by including the unscattered (ballistic) light into the description.

A more quantitative error analysis of the net flux at the interface at $z=0$ is displayed in Table I, where we compute the percentage error relative to the exact solution obtained from the MC simulations for the three models. The table indicates that the VHS model is always better than the PB solution at the surface and thus it seems ideal for a surface scanning based imaging. The predictions of the EB solution are erratic; for certain parameters they are better while for others they are worse than the PB solution.

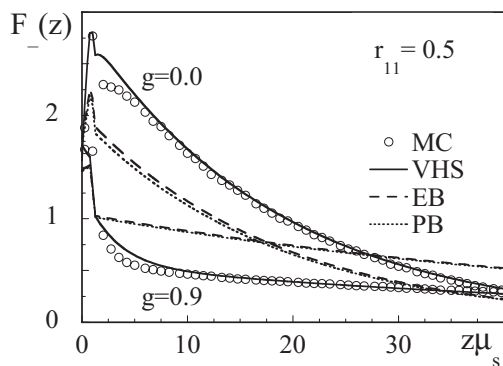


FIG. 4. Same quantities as Fig. 3, however, $r_{11}=0.5$. For the VHS model we chose $f_0=2.05$ ($g=0$) and $f_0=1.73$ ($g=0.9$). (Same source and medium parameters as in Fig. 2.)

TABLE I. The percentage error in the net output flux for various models at the interface at $z=0$ when compared to the exact solution obtained from the MC simulations for a medium with $\mu_a = 0.001\mu_s$.

	Percentage error in output flux at $z=0$			
	$r_{11}=0.25$		$r_{11}=0.50$	
	$g=0$	$g=0.9$	$g=0$	$g=0.9$
VHS	0.86%	2.2%	0.2%	3.85%
PB	4.0%	4.2%	9.4%	11.34%
EB	7.83%	1.9%	13.6%	10.5%

VI. DISCUSSION

We have extended the velocity half-sphere (VHS) model for infinite media to handle also systems with finite size and reflecting interfaces. There are two major improvements obtained from this approach. First, in contrast to the traditional diffusion equation one does not require any extrapolated boundary condition. The diffusion theory relies on extrapolation procedures to determine the location of these boundaries. These depend on various scattering parameters making this concept less practical for media with position dependent scattering and absorption coefficients. It is also inaccurate for highly forward scattering media because the usual phase function in the diffusion theory cannot be corrected by the δ -Eddington form as in the VHS model. The regions close to anisotropic sources cannot be modeled and the extrapolation procedure leads to a serious problem with regard to the conservation of the photon half flux. Second, the VHS model can incorporate the effect of highly reflecting interfaces much more accurately than the diffusion approaches, potentially opening up new avenues to develop imaging schemes using mirrors [25].

A limitation of the present work is that we provide VHS solution in terms of half-fluence $\Phi_+(\rho, z=0^+)$ which is generally not known in advance. On the other hand, an advantage of the boundary conditions used in this work is that the solutions are fairly general and should be applicable to a wide variety of interfaces. In special cases, when nonzero specular reflection is considered an approximate reflection function, $R(\Omega, \Omega')$ can be obtained from Fresnel relations. A solution can be obtained which only requires the knowledge of matrix elements r_{11} , r_{12} , r_{21} , and r_{22} . In future work, we plan to compare such a solution with MC simulation and study the different impact of specular and nonspecular reflecting interfaces.

Apart from applications in medical diagnostics and imaging, this model can be used in other areas such as nuclear engineering, atmospheric physics, oceanography [26], and seismic wave detection [27,28], where the radiative transfer theory is used extensively to describe boundary effects.

ACKNOWLEDGMENTS

This work has been supported by the NSF, Research Corporation, and BLV.

APPENDIX A

Here we derive the solutions (3.2) and (3.3) for the diffusion equation. The two moments $\Phi_d(\mathbf{r}) \equiv \int d\Omega I_d(\mathbf{r}, \Omega)$ and $\mathbf{J}_d(\mathbf{r}) \equiv \int d\Omega \Omega I_d(\mathbf{r}, \Omega)$ are insufficient to describe the dynamics near a boundary where the light distribution is highly anisotropic. The diffusion equation is obtained by integrating Eq. (2.1) over $\int d\Omega$ and over $\int \Omega d\Omega$. As a result the continuity equation $\nabla \cdot \mathbf{J}_d(\mathbf{r}) = -\mu_a \Phi_d(\mathbf{r}) + q \delta(x) \delta(y) \delta(z - z_s)$, and Fick's Law $\nabla \Phi_d(\mathbf{r})/3 = -(\mu_T - g\mu_s) \mathbf{J}_d(\mathbf{r}) + \mathbf{e}_z q \Delta \delta(x) \delta(y) \delta(z - z_s)/2$, can be obtained, respectively, where \mathbf{e}_z is the unit vector along the z axis. These two coupled equations can be reduced to the standard diffusion equation for the fluence $\Phi_d(\mathbf{r})$ as given in Eq. (3.1). We give here more a detailed derivation and discussion how various boundary conditions are implemented into the diffusion model. The usual diffusion equation (3.1) has the general (nondiverging) solution for $\Phi_d(\mathbf{r})$ given by the sum of the homogenous and a special solution

$$\begin{aligned} \Phi_d(\mathbf{r}) = & \int_0^\infty d\lambda A_\lambda \lambda J_0(\lambda \rho) \exp[-\alpha_\lambda(z + z_s)] / (4\pi D \alpha_\lambda) \\ & + \int_0^\infty d\lambda \lambda J_0(\lambda \rho) \{q/D - 3q_\Delta \partial_z/2\} \\ & \times \exp(-\alpha_\lambda|z - z_s|) / (4\pi \alpha_\lambda), \end{aligned} \quad (\text{A1})$$

where $J_0(\lambda \rho)$ is the zeroth order Bessel function, $\rho \equiv \sqrt{(x^2 + y^2)}$ and $\alpha_\lambda \equiv \sqrt{(\alpha^2 + \lambda^2)}$. For an isotropic point source ($q_\Delta = 0$) the special solution simplifies to the best known form $\Phi_d(\mathbf{r}) = \exp(-\alpha|\mathbf{r} - z_s \mathbf{e}_z|) / (4\pi D |\mathbf{r} - z_s \mathbf{e}_z|)$. Since some of the boundary conditions discussed in the text involve the flux, we also give here its general form $\mathbf{J}_d(\mathbf{r}) = J_{d\rho}(\mathbf{r}) \mathbf{e}_\rho + J_{dz}(\mathbf{r}) \mathbf{e}_z = -D(\partial_\rho \mathbf{e}_\rho + \partial_z \mathbf{e}_z) \Phi_d(\mathbf{r}) + 3D \mathbf{e}_z q_\Delta \delta(x) \delta(y) \delta(z - z_s)/2$ which follows from Fick's law

$$\begin{aligned} J_{d\rho}(\mathbf{r}) = & \int_0^\infty d\lambda A_\lambda \lambda^2 J_1(\lambda \rho) \exp[-\alpha_\lambda(z + z_s)] / (4\pi \alpha_\lambda) \\ & + \int_0^\infty d\lambda \lambda^2 J_1(\lambda \rho) (q - 3D q_\Delta \partial_z/2) \\ & \times \exp(-\alpha_\lambda|z - z_s|) / (4\pi \alpha_\lambda), \end{aligned} \quad (\text{A2a})$$

$$\begin{aligned} J_{dz}(\mathbf{r}) = & \int_0^\infty d\lambda A_\lambda \lambda J_0(\lambda \rho) \exp[-\alpha_\lambda(z + z_s)] / (4\pi) \\ & - \int_0^\infty d\lambda \lambda J_0(\lambda \rho) (q \partial_z / \alpha_\lambda - 3D \alpha_\lambda q_\Delta / 2) \\ & \times \exp(-\alpha_\lambda|z - z_s|) / (4\pi). \end{aligned} \quad (\text{A2b})$$

As we show below depending on the choice of the boundary condition, the set of expansion coefficients A_λ can be determined. The above solutions can be used to study both isotropic and certain types of anisotropic sources, but they are usually studied in the context of an isotropic source. However, light ejected from a fiber is anisotropic and can be modeled better as a half-source ($q_+ = 1, q_- = 0$). Such a correction can be significant when the source is close to the

boundary and measurements are made near this boundary. Below we briefly review the three most commonly used boundary conditions.

Zero boundary condition. The easiest boundary condition $\Phi_d(x, y, z=0) = 0$, is often used to model experimental data [29]. This solution (denoted with an additional subscript 0) is characterized by expansion coefficients $A_{\lambda 0} = -(q - 3D \alpha_\lambda q_\Delta / 2)$, for which the integral over λ can be performed analytically leading to

$$\begin{aligned} \Phi_{d0}(\mathbf{r}) = & -(q/D + 3q_\Delta \partial_z/2) \exp(-\alpha|\mathbf{r} + z_s \mathbf{e}_z|) / (4\pi |\mathbf{r} + z_s \mathbf{e}_z|) \\ & + (q/D - 3q_\Delta \partial_z/2) \exp(-\alpha|\mathbf{r} - z_s \mathbf{e}_z|) / (4\pi |\mathbf{r} - z_s \mathbf{e}_z|). \end{aligned} \quad (\text{A3})$$

The first term of this equation can be associated with the fluence of an imaginary antisource (photon sink) located at $\mathbf{r} = (0, 0, -z_s)$, similar to the inclusion of image charges in the corresponding electrostatics problems.

Partial current boundary condition. If there is no reflection at the boundary, the partial current condition assumes that the average incoming flux is equal to zero at $z=0$, i.e., $\int_+ d\Omega \cos \theta I_d(\mathbf{r}, \Omega) = 0$. This condition would be sufficient if $I_d(\mathbf{r}, \Omega)$ were always positive as required by the definition of the irradiance. However, the truncated expansion of $I_d(\mathbf{r}, \Omega)$ does not automatically guarantee a positive irradiance and thus the solution based on this condition is still bound to certain limitations. In the presence of reflection, defined via the coefficient $r_{11} \equiv -[\int_+ d\Omega \cos \theta I_d(\mathbf{r}, \Omega)] / [\int_- d\Omega \cos \theta I_d(\mathbf{r}, \Omega)]$, this condition leads to $(1 - 2D \gamma \partial_z) \Phi_{dP}(x, y, z=0) = 0$, where $\gamma \equiv (1 + r_{11}) / (1 - r_{11})$, and can be satisfied if the expansion coefficients take the form $A_{\lambda P} = -(1 - 2D \gamma \alpha_\lambda) (q - 3q_\Delta D \alpha_\lambda / 2) / (1 + 2D \gamma \alpha_\lambda)$. After some simplifications we arrive at the following solution for fluence [Eq. (3.2)]:

$$\begin{aligned} \Phi_{dP}(\mathbf{r}) = & \gamma (q + 3q_\Delta D \partial_z/2) \int_0^\infty d\lambda \lambda J_0(\lambda \rho) \exp[-\alpha_\lambda(z \\ & + z_s)] / [\pi(1 + 2D \gamma \alpha_\lambda)] - (q/D + 3q_\Delta \partial_z/2) \exp(-\alpha|\mathbf{r} \\ & - z_s \mathbf{e}_z|) / (4\pi D |\mathbf{r} + z_s \mathbf{e}_z|) + (q/D - 3q_\Delta \partial_z/2) \exp(-\alpha|\mathbf{r} \\ & - z_s \mathbf{e}_z|) / (4\pi D |\mathbf{r} - z_s \mathbf{e}_z|). \end{aligned} \quad (\text{A4})$$

Extrapolated boundary condition. The PB condition $(1 - 2D \gamma \partial_z) \Phi_{dP}(x, y, z=0) = 0$, can be viewed as the first two terms of the Taylor expansion of $\Phi(x, y, z - 2\gamma D)$ around z , thus we can write $(1 - 2D \gamma \partial_z) \Phi_{dP}(\mathbf{r}) \approx \Phi_{dP}(x, y, z - 2\gamma D)$. Consequently, if D is sufficiently small, we can approximate the partial current condition as $\Phi_{dP}(x, y, -2\gamma D) = 0$. Thus the fluence can be set equal to zero at an extrapolated plane at $z = -2\gamma D$. For a highly scattering medium (small D) with negligible reflection from the boundary ($\gamma \rightarrow 1$), the predictions of partial current condition and the extrapolated condition are similar [17]. By comparing this condition with the Milne problem the extrapolated boundary for an index matched medium ($\gamma = 1$) can be shifted from $z = -2D$ to $z = -2.131D$ [22]. We will denote this type of solution with an additional subscript E and the expansion coefficients are given by $A_{\lambda E} = -\exp(-\alpha_\lambda 4.262 \gamma D)$ leading to Eq. (3.3)

$$\begin{aligned} \Phi_{dE}(\mathbf{r}) = & -(q/D + 3q_{\Delta}\partial_z/2)\exp[-\alpha|\mathbf{r} + (z_s \\ & + 4.262\gamma D)\mathbf{e}_z|]/[4\pi D|\mathbf{r} + (z_s + 4.262\gamma D)\mathbf{e}_z|] + (q/D \\ & - 3q_{\Delta}\partial_z/2)\exp(-\alpha|\mathbf{r} - z_s\mathbf{e}_z|)/(4\pi D|\mathbf{r} - z_s\mathbf{e}_z|). \end{aligned} \quad (\text{A5})$$

APPENDIX B

In this appendix we show that the Milne problem predicts a discontinuity in $\Phi_+(\rho, z)$ at the medium's boundary, i.e., $\partial_z\Phi_+(\rho, z) \rightarrow \infty$ as $z \rightarrow 0$. The Milne problem is characterized by a semi-infinite medium ($z \geq 0$) and an infinitely extended source located at the plane $z = z_s$ such that the transverse effects can be neglected. Since the jump in $\Phi_+(\rho, z)$ is not affected by absorption we assume $\mu_a = 0$. A formal solution for the radiance is given by [22]

$$\begin{aligned} I_+(z, \cos \theta) = & \int_0^z \Phi(z') \exp[(z' - z)/\cos \theta] / (2 \cos \theta) dz' \\ & + \Theta(z - z_s) \exp\{(z_s - z)/\cos \theta\} / (2 \cos \theta), \\ & 0 < \cos \theta \leq 1, \end{aligned} \quad (\text{B1})$$

$$\begin{aligned} I_-(z, \cos \theta) = & - \int_z^\infty \Phi(z') \exp[(z' - z)/\cos \theta] / (2 \cos \theta) dz' \\ & - \Theta(z_s - z) \exp[(z_s - z)/\cos \theta] / (2 \cos \theta) \\ & - 1 \leq \cos \theta < 0, \end{aligned} \quad (\text{B2})$$

where z is here a dimensionless length measured in the units of $1/\mu_s$. If the source is located at infinity the source term is zero and the density $\Phi(z)$ satisfies the integral equation

$$\Phi(z) = \int_0^\infty dz' \Phi(z') \int_1^\infty dy \exp(-|z' - z|y)/y. \quad (\text{B3})$$

Integrating both equations (B1) and (B2) with respect to $\cos \theta$ and differentiating with respect to z we obtain

$$\begin{aligned} \partial_z \Phi_+(z) = & \Phi(z) \int_1^\infty dy / (2y) - \int_0^z \Phi(z') \exp[-(z - z')] / [2(z \\ & - z')] dz', \end{aligned} \quad (\text{B4})$$

$$\begin{aligned} \partial_z \Phi_-(z) = & - \Phi(z) \int_1^\infty dy / (2y) + \int_z^\infty \Phi(z') \exp[-(z' - z)] / [2(z' \\ & - z)] dz'. \end{aligned} \quad (\text{B5})$$

If we assume that the total fluence $\Phi(z)$ is nonzero at the boundary $z=0$ then the second term in Eq. (B4) is negligible in the limit $z \rightarrow 0$ and we obtain $\partial_z \Phi_+(z) \rightarrow \infty$. This conclusion for the Milne problem can be extended to other situations involving plane boundaries.

This discontinuity in $\Phi_+(\mathbf{r})$ leads to a discontinuity in $I(\mathbf{r}, \Omega)$ at the boundary as well [2] because of the definition $\Phi_+(\mathbf{r}) \equiv \int_+ d\Omega I(\mathbf{r}, \Omega)$. If $I(\mathbf{r}, \Omega)$ is discontinuous at the boundary then it must contain a term proportional to $\Theta(z)\delta(\cos \theta)$ [otherwise the operator $\Omega \cdot \nabla$ will give rise to $\delta(z)$ which is not present on the right-hand side of Eq. (2.1)] which cannot be expressed by a linear expansion in Ω given by Eq. (4.1). This problem of discontinuity in $\Phi_+(\mathbf{r})$ can be avoided by imposing the boundary condition slightly inside the medium at $z=0^+$ instead of $z=0$.

-
- [1] S. Chandrasekhar, *Radiative Transfer* (University Clarendon Press, Oxford, 1950).
- [2] M. M. R. Williams, *Mathematical Methods in Particle Transport Theory* (Wiley-Interscience, New York, 1971).
- [3] A. Ishimaru, *Wave Propagation and Scattering in Random Media* (Academic, New York, 1978), Vols. 1 and 2.
- [4] W. M. Star, in *Optical-Thermal Response of Laser-Irradiated Tissue*, edited by A. J. Welch and M. J. C. van Gemert (Plenum, New York, 1995), p. 131.
- [5] See articles in, *Optical Biomedical Diagnostics*, edited by V. V. Tuchin (SPIE, Bellingham, 2002).
- [6] M. C. W. van Rossum and T. M. Nieuwenhuizen, *Rev. Mod. Phys.* **71**, 313 (1999).
- [7] A. Yodh and B. Chance, *Phys. Today* **48**, 34 (1995).
- [8] A. H. Hielscher, A. Y. Bluestone, G. S. Abdoulaev, A. D. Klose, J. Lasker, M. Stewart, I. Netz, and J. Beuthan, *Dis. Markers* **18**, 313 (2002).
- [9] B. B. Das, F. Liu, and R. R. Alfano, *Rep. Prog. Phys.* **60**, 227 (1997).
- [10] V. Venugopalan, J. S. You, and B. J. Tromberg, *Phys. Rev. E* **58**, 2395 (1998); C. K. Hayakawa, B. Y. Hill, J. S. You, F. Bevilacqua, J. Spanier, and V. Venugopalan, *Appl. Opt.* **43**, 4677 (2004).
- [11] S. Menon, Q. Su, and R. Grobe, *Opt. Lett.* **30**, 1542 (2005).
- [12] S. Menon, Q. Su, and R. Grobe, *Phys. Rev. Lett.* **94**, 153904 (2005).
- [13] E. L. Hull and T. H. Foster, *J. Opt. Soc. Am. A* **18**, 584 (2001).
- [14] R. Aronson, *J. Opt. Soc. Am. A* **12**, 2532 (1995).
- [15] L. H. Wang, S. L. Jacques, and L. Q. Zheng, *Comput. Methods Programs Biomed.* **47**, 131 (1995).
- [16] A. H. Hielscher, S. L. Jacques, L. Wang, and F. K. Tittel, *Phys. Med. Biol.* **40**, 1957 (1995).
- [17] R. C. Haskell, L. O. Svaasand, T. T. Tsay, T. C. Feng, M. S. McAdams, and B. J. Tromberg, *J. Opt. Soc. Am. A* **11**, 2727 (1994).
- [18] M. U. Vera and D. J. Durian, *Phys. Rev. E* **53**, 3215 (1996).
- [19] D. J. Durian, *Phys. Rev. E* **50**, 857 (1994).
- [20] M. Lax, V. Nayaranamurti and R. C. Fulton, in *Proceedings of the Symposium on Laser Optics of Condensed Matter, Leningrad, June 1987*, edited by J. L. Birman, H. Z. Cummins, and A. A. Kaplyanskii (Plenum, New York, 1987).
- [21] K. M. Yoo, F. Liu, and R. R. Alfano, *Phys. Rev. Lett.* **64**, 2647 (1990).
- [22] P. Morse and H. Feshbach, *Methods of Theoretical Physics* (McGraw Hill, New York, 1953), Vols. I and II.

- [23] S. Menon, Q. Su, and R. Grobe, *Phys. Rev. E* **72**, 041910 (2005).
- [24] M. Born and E. Wolf, *Principles of Optics*, 7th ed. (Cambridge University Press, Cambridge, 1999).
- [25] R. Wenning, Q. Su, and R. Grobe, *Laser Phys.* **16**, 631 (2006).
- [26] G. E. Thomas and K. Stamnes, *Radiative Transfer in the Atmosphere and Ocean* (Cambridge University Press, Cambridge, 2002).
- [27] R. S. Wu, *Geophys. J. R. Astron. Soc.* **82**, 57 (1985).
- [28] M. Fehler and H. Sato, *Pure Appl. Geophys.* **160**, 541 (2003).
- [29] M. S. Patterson, B. Chance, and B. C. Wilson, *Appl. Opt.* **28**, 2331 (1989).